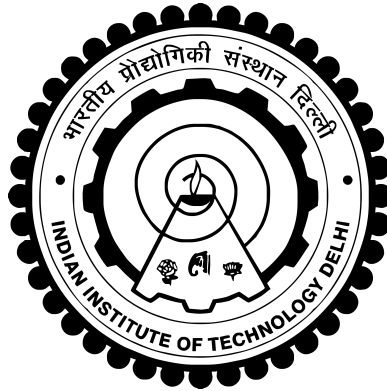


Compact and Wide Beamwidth Filtering Antennas for High Power Applications

Dristi Singhal



INDIAN INSTITUTE OF TECHNOLOGY DELHI
HAUZ KHAS, NEW DELHI-110016, INDIA

March, 2025

© **Indian Institute of Technology Delhi (IITD), New Delhi, 2025**

**Compact and Wide Beamwidth Filtering Antennas
for High Power Applications**

by

Dristi Singhal

Centre for Applied Research in Electronics

Submitted

In fulfillment of the requirements of the degree of

Doctor of Philosophy

to the



INDIAN INSTITUTE OF TECHNOLOGY DELHI

HAUZ KHAS, NEW DELHI-110016, INDIA

March, 2025

CERTIFICATE

This is to certify that the thesis titled "**Compact and Wide Beamwidth Filtering Antennas for High Power Applications**", being submitted by **Mrs. Dristi Singhal**, to the **Indian Institute of Technology Delhi**, for the award of the degree of **Doctor of Philosophy**, is a record of the bonafide research work carried out by her. She has worked under my supervision and guidance and has fulfilled the requirements, which to my knowledge, have reached the requisite standard for the submission of the thesis. The results presented in this thesis have not been submitted in part or full for the award of any degree or diploma in any other University or Institute.

Dr. Kirti Dhvaj
Assistant Professor
Centre for Applied Research in Electronics
Indian Institute of Technology Delhi
Hauz Khas, New Delhi-110016, India

ACKNOWLEDGEMENTS

First and foremost, I would like to express my sincere gratitude and deep appreciation to my supervisor, **Dr. Kirti Dhwaj**, for the invaluable opportunity to carry out my doctoral research under his guidance. It has been a true privilege to learn and grow under his mentorship, and I find it challenging to fully convey my appreciation. During my Ph.D., **Dr. Kirti Dhwaj** introduced me to the exciting field of microwave filters and filtering antennas, a field that has profoundly influenced my professional career. Throughout my research, his constant support, encouragement, and deep knowledge have made a huge difference to this work. Simultaneously, his mentorship, creative insights, and comprehensive knowledge laid the essential foundation for this work. I am also very thankful for the freedom he allowed me, which helped me achieve publishable results in a short time. His ability to assess the novelty of my research was consistently accurate, and I am especially grateful to him for teaching me the process of crafting an effective journal paper from scratch.

I am indebted to my SRC members, **Prof. Ananjan Basu**, **Prof. Mahesh P Abegaonkar**, and **Prof. Shouribrata Chatterjee**, for their unwavering support and insightful ideas during my project. I'd like to express my gratitude to **Mr. Sanjay Singh** from Production Engineering Lab and **Mr. Roshanlal** of the central workshop for assisting me in fabricating intricate structures using an in-house fabrication facility. I am deeply thankful to the **Ministry of Human Resource Development (MHRD)** for awarding me the Research Fellowship and providing financial support throughout my Ph.D.

I would like to express my gratitude to my friends Mohit Agarwal and Madhur Pandya for their constant support and assistance during my Ph.D., most importantly with the fabrication of microwave components using in-house fabrication facility. I would like to express my heartfelt gratitude to all members of the Microwave Group, Mr. Ashok, Mr. Sanjeev, Shakti Singh Chauhan, Pranav Shrivastava, Somia Sharma, Shilpi Singh, Ratul De, Vijoyatry Paul, Rupa Laller, Tanvi Agarwal, Aditya Kumar Thakur, Pawan Kumar, Faheem

Firdoush, Devesh Pratap Singh, and Aman Raj for their steadfast support, assistance, and encouragement throughout my Ph.D. journey.

It's a little tough to mention everyone who contributed to this accomplishment, whether directly or indirectly. Nonetheless, I would like to express my heartfelt gratitude to my husband, Mr. Abhay Agrawal for his care, motivation and constant support during the ups and downs of this journey and my life in general. My father-in-law, Mr. Manoj Kumar, mother-in-law, Mrs. Ruby Agarawal and brother-in-law, Mr. Ashrut Agrawal have also been a constant source of support and assisted me in various facets of my life.

I am forever grateful to my grandmother, Mrs. Ramrati Devi, my father, Mr. Pramod Kumar Singhal, my mother, Mrs. Ritu Singhal, and my brother, Mr. Ankush Singhal, for their constant support throughout my life. Their resilience and sacrifices have greatly influenced who I am today. They have always been there for me, providing endless love, care, motivation, and blessings. This achievement would not have been possible without their encouragement and unwavering support.

Finally, I extend my humble gratitude to **The Almighty God**, whose kindness and blessings have made it possible for me to complete this academic undertaking.

New Delhi

March 2025

Dristi Singhal

**Under the inspiration of Almighty God
I dedicate this thesis to my
Parents and Husband**

ABSTRACT

A filter placed before the radiating element is a crucial component in the front-end of communication systems, as it allows signals in the desired band to pass while suppressing those in unwanted bands. Traditionally, filters and antennas are designed separately and connected through a transmission line, which results in increased size and transition loss.

Evanescent-mode waveguide components offer medium to high power handling capability in a compact footprint with low loss characteristics. A small cross-section of evanescent-mode open-ended waveguide (EMOEW) plays an important role in electronic warfare systems and phased array systems as it provides wide beamwidths. However, the wave admittance of EMOEW is susceptible in nature, while its propagation constant is real; restricting the propagation of wave. On the other hand, the small aperture of EMOEW does not allow radiation of wave due to the presence of reflections at the aperture discontinuity.

This dissertation presents the solution by introducing the capacitive discontinuities inside the EMOEW such that in-band aperture matching and out-of-band filtering response can be achieved, simultaneously in a compact footprint. In the first work, two high-Q dielectric resonators (DRs) are mounted inside the EMOEW to provide matching to its small aperture along with high out-of-band selectivity. The small aperture of EMOEW is responsible for yielding a wide beam response with an appreciable gain value in a compact form factor. However, the proposed filtering antenna operates at only a single frequency with a particular bandwidth. As such, multiple antennas are required in front-end preselection for fixed spectrum multiband wireless communication systems.

A compact frequency reconfigurable filtering antenna is the second work that is being presented in this dissertation. It is useful not only for electronic warfare and phased array systems but also for cognitive radio systems and front-end preselection for fixed-spectrum multi-band wireless communication systems. The proposed reconfigurable filtering antenna operates at X-band and provides 10 % of frequency reconfigurability by maintaining the constant absolute bandwidth and constant realized gain capabilities. As the thermally stable

reconfigurable filtering antenna is developed using EMOEW, it yields wide beamwidths and high power handling capability. However, both static and reconfigurable filtering antennas exhibit reductions in areas but not in their lengths.

Length reduction along with reduced area can be achieved by using dual-mode resonators, dictating the third and the fourth work of the dissertation. A dual-mode dielectric resonator-loaded evanescent-mode waveguide-based filtering antenna is presented as the third work. Two transmission zeros are created at the upper side of the passband, defining the stopband bandwidth of the filtering antenna. This stopband bandwidth is reconfigured for adaptive cancellation of adjacent-channel interference. The proposed wide-beam filtering antenna is the smallest waveguide-based filtering antenna and provides transmission zeros in evanescent-mode waveguide technology. However, in this case, adjacent-channel interference can be suppressed only at the upper side of the passband.

In order to allow suppression of adjacent-channel interference both at the upper side and at the lower side of the passband, a quasi-elliptic response filtering antenna is ideally suited, which we are going to discuss as the fourth work of this dissertation. In this work, one of the transmission zeros of the third work is brought down at the lower side of the passband to allow high out-of-band suppression at both sides of the passband. To do so, an ellipsoid dual-mode dielectric resonator is utilized to allow radiation of wave in the passband with two transmission zeros (one at each side of the passband) in the stopband. This is an ultra-compact design with a quasi-elliptic response in the evanescent-mode waveguide. Additionally, the small aperture of EMOEW allows wide E-plane beamwidth with a reasonable gain value.

All the EMOEW-based filtering antennas - discussed in this dissertation - are thermally stable, making them useful for variety of high-power applications in a compact footprint, and can be scaled from microwave-to-mmWave frequency range.

सार

रेडिएटिंग तत्व के सामने रखा गया फ़िल्टर संचार प्रणालियों के फ्रंट-एंड में एक महत्वपूर्ण घटक है, क्योंकि यह वांछित बैंड में संकेतों को पारित करने की अनुमति देता है जबकि अवांछित बैंड में उन्हें दबा देता है। परंपरागत रूप से, फ़िल्टर और एंटेना अलग-अलग डिज़ाइन किए जाते हैं और ट्रांसमिशन लाइन के माध्यम से जुड़े होते हैं, जिसके परिणामस्वरूप आकार और संक्रमण हानि बढ़ जाती है।

इवेनसेंट-मोड वेवगाइड घटक कम हानि विशेषताओं के साथ एक कॉम्पैक्ट फुटप्रिंट में मध्यम से उच्च शक्ति हैंडलिंग क्षमता प्रदान करते हैं। इवेनसेंट-मोड ओपन-एंडेड वेवगाइड (EMOEW) का एक छोटा क्रॉस-सेक्शन इलेक्ट्रॉनिक युद्ध प्रणालियों और चरणबद्ध सरणी प्रणालियों में एक महत्वपूर्ण भूमिका निभाता है क्योंकि यह व्यापक बीमविड्थ प्रदान करता है। हालाँकि, EMOEW की तरंग प्रवेश प्रकृति में संवेदनशील है, जबकि इसका प्रसार स्थिरांक वास्तविक है; तरंग के प्रसार को प्रतिबंधित करता है। दूसरी ओर, EMOEW का छोटा एपर्चर एपर्चर असंततता पर प्रतिबिंबों की उपस्थिति के कारण तरंग के विकिरण की अनुमति नहीं देता है।

यह शोध प्रबंध EMOEW के अंदर कैपेसिटिव डिसकॉन्टिन्यूटी को पेश करके समाधान प्रस्तुत करता है, ताकि एक साथ इन-बैंड एपर्चर मैचिंग और आउट-ऑफ-बैंड फ़िल्टरिंग प्रतिक्रिया को एक कॉम्पैक्ट फुटप्रिंट में प्राप्त किया जा सके। पहले काम में, EMOEW के अंदर दो हाई-Q डाइइलेक्ट्रिक रेज़ोनेटर (DR) लगाए गए हैं ताकि उच्च आउट-ऑफ-बैंड चयनात्मकता के साथ-साथ इसके छोटे एपर्चर से मिलान किया जा सके। EMOEW का छोटा एपर्चर एक कॉम्पैक्ट फ़ॉर्म फैक्टर में एक सराहनीय लाभ मूल्य के साथ एक विस्तृत बीम प्रतिक्रिया देने के लिए ज़िम्मेदार है। हालाँकि, प्रस्तावित फ़िल्टरिंग एंटीना एक विशेष बैंडविड्थ के साथ केवल एक ही आवृत्ति पर काम करता है। इस प्रकार, फिक्स्ड स्पेक्ट्रम मल्टीबैंड वायरलेस संचार प्रणालियों के लिए फ्रंट-एंड प्रीसेलेक्शन में कई एंटेना की आवश्यकता होती है। एक कॉम्पैक्ट फ्रीक्वेंसी रीकॉन्फ़िगर करने योग्य फ़िल्टरिंग एंटीना दूसरा काम है जिसे इस शोध प्रबंध में प्रस्तुत किया जा रहा है, जो न केवल इलेक्ट्रॉनिक युद्ध और चरणबद्ध सरणियों के लिए उपयोगी है, बल्कि संज्ञानात्मक रेडियो प्रणालियों के साथ-साथ फिक्स्ड स्पेक्ट्रम मल्टी-बैंड वायरलेस संचार प्रणालियों के लिए फ्रंट-एंड प्रीसेलेक्शन के लिए भी उपयोगी है। प्रस्तावित पुनर्संयोज्य फ़िल्टरिंग एंटेना X-बैंड पर संचालित होता है और निरंतर निरपेक्ष बैंडविड्थ और निरंतर प्राप्त लाभ क्षमताओं को बनाए रखते हुए 10% आवृत्ति पुनर्संयोज्यता प्रदान करता है।

चूंकि थर्मली स्थिर पुनर्संयोज्य फ़िल्टरिंग एन्टेना को EMOEW का उपयोग करके विकसित किया गया है, इसलिए यह व्यापक बीमविद्युत और उच्च शक्ति हैंडलिंग क्षमता प्रदान करता है। हालाँकि, स्थिर और पुनर्संयोज्य फ़िल्टरिंग एन्टेना दोनों ही क्षेत्रों में कमी प्रदर्शित करते हैं, लेकिन उनकी लंबाई में नहीं।

दोहरे मोड वाले अनुनादकों का उपयोग करके लंबाई में कमी के साथ-साथ कम क्षेत्र प्राप्त किया जा सकता है, जो शोध प्रबंध के तीसरे और चौथे कार्य को निर्देशित करता है। दोहरे मोड वाले डाइइलेक्ट्रिक अनुनादक-लोडेड इवेनसेंट-मोड वेवगाइड-आधारित फ़िल्टरिंग एन्टेना को तीसरे कार्य के रूप में प्रस्तुत किया गया है। फ़िल्टरिंग एन्टेना के स्टॉपबैंड बैंडविद्युत को परिभाषित करते हुए पासबैंड के ऊपरी हिस्से में दो ट्रांसमिशन ज़ीरो बनाए जाते हैं। इस स्टॉपबैंड बैंडविद्युत को आसन्न-चैनल हस्तक्षेप के अनुकूली रद्दीकरण के लिए पुनर्संयोजित किया जाता है। प्रस्तावित वाइड-बीम फ़िल्टरिंग एन्टेना सबसे छोटा वेवगाइड-आधारित फ़िल्टरिंग एन्टेना है और इवेनसेंट-मोड वेवगाइड तकनीक में ट्रांसमिशन ज़ीरो प्रदान करता है। हालाँकि, इस मामले में, आसन्न-चैनल हस्तक्षेप को केवल पासबैंड के ऊपरी हिस्से पर ही दबाया जा सकता है।

पासबैंड के ऊपरी हिस्से और निचले हिस्से दोनों पर आसन्न-चैनल हस्तक्षेप को दबाने के लिए, एक अर्ध-अण्डाकार प्रतिक्रिया फ़िल्टरिंग एंटीना आदर्श रूप से उपयुक्त है, जिस पर हम इस शोध प्रबंध के चौथे कार्य के रूप में चर्चा करने जा रहे हैं। इस कार्य में, तीसरे कार्य के ट्रांसमिशन शून्य में से एक को पासबैंड के निचले हिस्से में लाया जाता है ताकि पासबैंड के दोनों किनारों पर उच्च आउट-ऑफ-बैंड दमन की अनुमति मिल सके। ऐसा करने के लिए, पासबैंड में तरंग के विकिरण की अनुमति देने के लिए गोलाकार दोहरे मोड ढांकता हुआ अनुनादक को दीर्घवृत्ताकार बनाया जाता है, जिसमें स्टॉपबैंड में दो ट्रांसमिशन शून्य (पासबैंड के प्रत्येक तरफ एक) होते हैं। यह एक अति-कॉम्पैक्ट डिज़ाइन है जिसमें वाष्पशील-मोड वेवगाइड में अर्ध-अण्डाकार प्रतिक्रिया होती है। इसके अतिरिक्त, EMOEW का छोटा एपर्चर एक उचित लाभ मूल्य के साथ विस्तृत E-प्लेन बीमविद्युत की अनुमति देता है।

सभी EMOEW-आधारित फ़िल्टरिंग एंटेना - जिनकी चर्चा इस शोध प्रबंध में की गई है - ऊष्मीय रूप से स्थिर हैं, जो उन्हें कॉम्पैक्ट फुटप्रिंट में विभिन्न प्रकार के उच्च-शक्ति अनुप्रयोगों के लिए उपयोगी बनाता है, और उन्हें माइक्रोवेव-से-एमएमवेव आवृत्ति रेंज में स्केल किया जा सकता है।

Contents

CERTIFICATE	i
ACKNOWLEDGEMENTS	ii
ABSTRACT	v
List of Figures	xx
List of Tables	xxi
1 INTRODUCTION	1
1.1 Filtering Antenna	1
1.2 Realization of Filtering Antenna	2
1.3 Compact and High Power Filtering Antennas with Wide Beamwidths	6
1.3.1 Reducing length, l	7
1.3.2 Reducing Cross-sectional Area, $a \times b$	7
1.4 Relevance of Wide Beamwidth in High Power Applications	10
1.4.1 Airborne Radars	10
1.4.2 Spaceborne SARs	11
1.4.3 Phased Arrays	12
1.5 Motivation	12
1.6 Scope and Objective	15
1.7 Organization of the Thesis	16
2 EVANESCENT-MODE FILTERING ANTENNA	18
2.1 Introduction	18
2.2 Proposed Evanescent-Mode Filtering Antenna	21

2.2.1	Synthesis of Filtering Antenna	22
2.2.2	Physical development of filtering Antenna	23
2.3	Simulated and Measured Responses	28
2.4	Power Handling Analysis	31
2.5	Comparison of Filtering Antennas	32
2.6	Conclusion	33
3	FREQUENCY RECONFIGURABLE FILTERING ANTENNA	34
3.1	Introduction	34
3.2	Proposed RFA	36
3.2.1	Synthesis of RFA	38
3.2.2	Physical Realization of CABW RFA	39
3.2.3	CRG Tuning	44
3.3	Simulated and Measured Responses of RFA	45
3.4	Power Handling Analysis	49
3.4.1	Multipactor Breakdown Analysis	49
3.4.2	Thermal Analysis	49
3.5	Comparison of RFAs	51
3.6	Conclusion	51
4	FILTER/FILTERING ANTENNA WITH TUNABLE STOPBAND BAND- WIDTH	52
4.1	Introduction	52
4.2	Dual-Mode Filter	56
4.2.1	Design	56
4.2.2	Simulated and Measured Responses	62
4.3	Dual-Mode Filtering Antenna	64
4.3.1	Design	64
4.3.2	Simulated and Measured Responses of Filtering Antenna	67
4.4	Power Handling Analysis	70
4.4.1	Multipactor Breakdown Analysis	71
4.4.2	Thermal Analysis	71

4.5	Comparison of Waveguide Filtering Antennas	73
4.6	Conclusion	74
5	COMPACT FILTERING ANTENNA WITH QUASI-ELLIPTIC RE- SPONSE	75
5.1	Introduction	75
5.2	Proposed Evanescent-Mode Filtering Antenna	77
5.2.1	Design	77
5.2.2	Development of Filtering Antenna	78
5.3	Simulation and Measurement Responses	86
5.4	Power Handling Analysis	87
5.4.1	Thermal Analysis	88
5.5	Comparison of Filtering Antennas	90
5.6	Conclusion	91
6	Conclusions and suggestions for future research	92
6.1	Conclusion	92
6.2	Future Scope	93
	References	94
	Appendix A	101
	Brief biodata and Publications	106

List of Figures

1.1	Block diagram of the front-end of communication systems with (a) a filter and an antenna connected through a transmission line. (b) a co-designed filtering antenna.	2
1.2	Network representation of an n pole filtering antenna and its radiating aperture.	5
1.3	Equivalent network representation of the n pole filtering antenna with its radiating aperture.	5
1.4	3D view of an OEW.	7
1.5	(a) θ_H of the OEW for different values of a and fixed values of $b = 0.34\lambda_0$ and $l = 0.95\lambda_0$. (b) θ_E of the OEW for different values of b and fixed values of $a = 0.42\lambda_0$ and $l = 0.95\lambda_0$. Here, OEW is fed by a WR-112 waveguide.	8
1.6	Radiated power response of the OEW with $a = 0.42\lambda_0$, $b = 0.34\lambda_0$ and $l = 0.95\lambda_0$. Also, $f_c^{Ev} = 9.61$ GHz is the cut-off frequency of OEW. The input power spectral density to the OEW is uniformly 1 W/Hz across the frequency range.	9
1.7	Radiated power responses of the OEW. Illustrating the reduction in radiated power level below f_c , with b varying from $0.34\lambda_0$ to $0.26\lambda_0$ for fixed values of $a = 0.42\lambda_0$ and $l = 0.95\lambda_0$. Also, the input power spectral density to the OEW is uniformly 1 W/Hz across the frequency range.	10

1.8	Shown here is the side view of airborne radar mounted on aircraft. It can be seen that as the beamwidth of antenna increases a large number of targets can be detected compared to the narrow beam of the antenna, leading to reduced search time of targets.	11
1.9	Representation of a SAR system.	11
1.10	Radiation patterns of phased array system at different angles and its unit element at 0° in rectangular plot.	12
1.11	Cross-sectional view of (a) propagating-mode OEW and (b) EMOEW. Here, λ_0 is the free space wavelength at operating frequency, f_0 . For propagating-mode OEW, $f_0 > f_c$ and for EMOEW, $f_0 < f_c$	13
2.1	Top-view of the EMOEW fed by a propagating-mode WR-112 waveguide, with its lumped equivalent circuit at f_0 . Here, $Y_S = G_S + jB_S$ and $Y_A = G_A + jB_A$ are the source and the aperture admittances, respectively. G_S is the conductance of port, while B_S is the susceptance at WR-112 and EMOEW interface (or at the step discontinuity). G_A and B_A are the conductance and the susceptance at the aperture discontinuity, respectively. The T-network of L_1 , L_2 and L_3 is used to denote the reactive nature of EMOEW.	19
2.2	Radiated power response of the OEW with $a = 0.42\lambda_0$, $b = 0.26\lambda_0$ and $l = 0.95\lambda_0$. The input power spectral density to the OEW is uniformly 1 W/Hz across the frequency range.	19
2.3	Top-view of a radiating EMOEW fed by a propagating mode WR-112 waveguide, with its lumped equivalent circuit at f_0 . Here, a lumped capacitance (C_2) is placed along the length of EMOEW to allow propagation of wave. The presence of C_2 also allows for radiation from the small aperture of EMOEW.	20
2.4	(a) Longitudinal view of evanescent-mode waveguide filtering antenna. Both DRs are identical. (b) Schematic of a DR. The relevant dimensions are: $l_{ew} = 34.3 \text{ mm}$, $l_{12} = 20 \text{ mm}$, $l_{S1} = 5 \text{ mm}$, $l_{2L} = 9.3 \text{ mm}$, $H_R = 6.8 \text{ mm}$, $H_S = 4 \text{ mm}$, $D_R = 9.5 \text{ mm}$, $D_S = 4 \text{ mm}$	22

2.5	Coupling scheme of proposed second order filtering antenna. Parameters are given as: $f_1 = 8$ GHz, $f_2 = 7.98$ GHz, $Q_{S1} = 30.47$, $Q_{2L} = 40$, $K_{12} = 0.03$.	23
2.6	(a) Circuit representation of DR_2 and radiating aperture. (b) Equivalent resonator representation of DR_2 with radiating aperture.	24
2.7	Variation of f_2 with l_{2L}	25
2.8	Setup for eigenmode solution of DR_2	25
2.9	Variation of Q_{S1} with l_{S1}	26
2.10	Variation of Q_{2L} with l_{2L}	27
2.11	Variation of K_{12} with l_{12}	27
2.12	Photographs of fabricated evanescent-mode filtering antenna: (a) Cross-sectional view of the filtering antenna with top-cover removed. (b) Composite view of filtering antenna with coax-to-waveguide adapter.	29
2.13	Frequency response of the filtering antenna.	30
2.14	Simulated end-fire realized gain variation of EMOEW without DRs.	30
2.15	Radiation patterns of filtering antenna at f_0 in (a) E-plane and (b) H-plane.	31
2.16	Configuration for multipactor breakdown analysis.	31
3.1	(a) Model representation of a filter. (b) Model representation of a reconfigurable filter.	34
3.2	(a) Model representation of a filter and an antenna connected through a transmission line. (b) Model representation of a co-designed filtering antenna. (c) Model representation of a frequency reconfigurable co-designed filtering antenna, attesting to reduction in size and cost of the filtering antenna.	35

3.3	(a) Longitudinal view of waveguide RFA. Stepped screws are shown outside the slot of ring-shaped DRs. Both the DRs as well as both the stepped screws are identical. (b) Schematic of a DR with the stepped screw inserted in the slot of DR. (C) Top view of the DR. The relevant dimensions are: $l_w = 10$ mm, $l_{ew} = 34.3$ mm, $l_{S1} = 5.1$ mm, $l_{12} = 20$ mm, $l_{2L} = 9.2$ mm, $H_R = 6.8$ mm, $H_S = 4$ mm, $D_{R0} = 9.5$ mm, $D_{R1} = 3.5$ mm, $D_S = 6$ mm, $D_{T0} = 9$ mm, $D_{T1} = 3$ mm, $l_{T1} = 4$ mm. The diameters of screws S_3 , S_4 and S_5 are 4 mm, 4 mm and 3 mm, respectively.	37
3.4	Coupling scheme of proposed second order RFA. Normalized parameters are given as: $M_{G1} = 1.0691$, $M_{2L} = 0.9168$, $M_{12} = 1.1087$. Both the DRs are synchronously tuned at f_0	38
3.5	(a) Isotropic view of ring-shaped DR. (b) Evanescent field distribution at XZ plane in the vicinity of DR. The fields are plotted at f_0	40
3.6	Variation of f_0 with total penetration of screw. For conventional screw, $D_{T0} = D_{T1} = 3$ mm. For both screws, $l_{T1} = 4$ mm.	41
3.7	Variation of Q_{G1} with f_0	41
3.8	(a) Circuit representation of DR_2 and radiating aperture. (b) Equivalent resonator representation of DR_2 with radiating aperture.	42
3.9	Setup for eigenmode solution of DR_2 in HFSS.	42
3.10	Variation of Q_{2L} with f_0	43
3.11	Variation of K_{12} with f_0	43
3.12	Variation of simulated efficiency, simulated absolute magnitude of directivity and simulated absolute magnitude of realized gain with f_0	44
3.13	Photographs of fabricated RFA: (a) Longitudinal view with coax-to-waveguide adapter. (b) Cross-sectional view with aperture.	45
3.14	Responses of RFA at T_A , T_B and T_C : (a) S_{11} and (b) end-fire realized gain.	47
3.15	Simulated end-fire realized gain of EMOEW without DRs.	48

3.16	Radiation patterns of RFA in (a) T_A at f_0 with beamwidths 80° in E-plane and 78° in H-plane, (b) T_B at f_0 with beamwidths 90° in E-plane and 70° in H-plane and (c) T_C at f_0 with beamwidths 95° in E-plane and 80° in H-plane.	48
3.17	Configuration for multipactor breakdown analysis.	49
3.18	Simulated variations of f_0 and realized gain of RFA in state T_C at different temperatures.	50
4.1	Block diagram for an inline configuration of two pole filtering antenna using (a) two single mode resonators and (b) a dual-mode resonator. Here, d is the centre-to-centre distance between the two physical resonators.	53
4.2	Frequency response of a high-Q bandpass filter, indicating the passband region around f_1 and suppression of signals in the stopband when (a) there are no transmission zeros in the stopband. (b) there are two transmission zeros at the upper side of the passband, which defines the stopband bandwidth of the filter and allows suppression of nearby channels at frequency, f_2 . (c) the stopband bandwidth of the filter is tuned (or increased) to suppress nearby channels with wider bandwidth at f_2	55
4.3	(a) Top view of the L-shaped evanescent-mode waveguide dual-mode filter. (b) Top view of filter, showing the plane of symmetry. (c) Cross-sectional view of the filter on the plane of symmetry. Here, steel screw is used to reconfigure the stopband bandwidth. The relevant dimensions are: $L_{ew} = 22.2 \text{ mm}$, $L_S = L_L = 14.3 \text{ mm}$, $L_P = 11.2 \text{ mm}$, $L_{SP} = 6.3 \text{ mm}$, $L_{ST} = 5.4 \text{ mm}$, $H_R = 6.4 \text{ mm}$, $D_R = 7.6 \text{ mm}$, $S_D = 3 \text{ mm}$. S_L is variable in length.	57
4.4	Magnitude of electric field distribution in a DMDR for degenerate modes: (a) the even mode (at f_{0e}) and (b) the odd mode (at f_{0o}). Shown here is the top view of DMDR.	58
4.5	Coupling scheme of the proposed second-order dual-mode filter. Parameters are given as: $Q_{Se} = 148$, $Q_{eLF} = 148$, $Q_{So} = 246$, $Q_{oLF} = -246$, $K_{eeF} = 1.24 \times 10^{-2}$, $K_{ooF} = -1.22 \times 10^{-2}$, $K_{SL} = 1.38 \times 10^{-4}$	58
4.6	Variation of (a) K_{eeF} with L_P and (b) K_{ooF} with L_P	59

4.7	Variation of (a) Q_{S_e} with L_S and (b) Q_{S_o} with L_S	61
4.8	(a) Frequency variations of synthesized S_{21} responses of the filter for different values of K_{SL} by keeping all other coupling parameters identical. (b) Variation of K_{SL} with S_L	62
4.9	Photographs of fabricated L-shaped dual-mode filter: (a) Cross-sectional view of the filter with top-cover removed. (b) Composite view with feeding adapters.	63
4.10	Frequency response of the proposed filter with tunable stopband bandwidth.	64
4.11	Top view of the L-shaped evanescent-mode waveguide-based dual-mode filtering antenna. Here, $D_R = 7.56 \text{ mm}$ and $L_L = 17 \text{ mm}$. All other dimensions of filtering antenna are identical to that of the filter shown in Fig. 4.3. . . .	65
4.12	(a) Circuit representation of DR_e of the filter and the step discontinuity between evanescent-mode and match-terminated propagating-mode load waveguides. Here, G_S is the conductance of port and B_S is the susceptance at step discontinuity. (b) Circuit representation of DR_e of the filtering antenna with aperture discontinuity.	65
4.13	(a) Circuit representation of DR_o of the filter and the step discontinuity between evanescent-mode and match-terminated propagating-mode load waveguides. Here, G_S is the conductance of port and B_S is the susceptance at step discontinuity. (b) Circuit representation of DR_o of the filtering antenna with aperture discontinuity.	65
4.14	(a) Circuit representation of DR_e of the filtering antenna and the aperture. (b) Equivalent resonator representation of DR_e of the filtering antenna with aperture. Here, $Q_{ue} = Q_{eLA}$	66
4.15	(a) Circuit representation of DR_o of the filtering antenna and the aperture. (b) Equivalent resonator representation of DR_o of the filtering antenna with aperture. Here, $Q_{uo} = Q_{oLA}$	67
4.16	Setup for eigenmode solver in HFSS.	67

4.17	Variations with L_L and D_R of (a) K_{eeA} and K_{ooA} , (b) Q_{ue} and Q_{uo}	68
4.18	Photograph of the filtering antenna: (a) Exploded view with top cover removed. (b) Aperture view.	69
4.19	Frequency response of the proposed filtering antenna with tunable stopband bandwidth.	70
4.20	Simulated end-fire realized gain of EMOEW without DMDR.	70
4.21	Radiation patterns of filtering antenna at f_0 in (a) E-plane and (b) H-plane.	71
4.22	Simulated frequency responses of filtering antenna in state T_A at different temperatures.	72
5.1	(a) Top view and (b) side view of a circular DMDR. Here, $D_1 = D_2$	77
5.2	(a) Magnitude of E-field distribution in the top view of an ellipsoid DMDR at f_{0o} . (b) Magnitude of E-field distribution in the top view of an ellipsoid DMDR at f_{0e}	78
5.3	Simulated variations of f_{0o} and f_{0e} with the ratios of major axis (D_2) and the minor axis (D_1) of ellipsoid DMDR, D_2/D_1 . Here, $D_1 = \text{constant} = 7.36 \text{ mm}$	78
5.4	(a) 3D-view of the proposed L-shaped evanescent-mode waveguide dual-mode filtering antenna. (b) Top view of the filtering antenna showing the diagonal plane. (c) Cross-sectional view on the diagonal plane. The relevant dimensions are: $L_{ew1} = 20.1 \text{ mm}$, $L_{ew2} = 22.9 \text{ mm}$, $L_S = 12.15 \text{ mm}$, $L_L = 14.95 \text{ mm}$, $L_P = 11.2 \text{ mm}$, $D_1 = 7.36 \text{ mm}$, $D_2 = 7.75 \text{ mm}$ and $b = 6.4 \text{ mm}$. Also, $f_c^{Ev} = 9.43 \text{ GHz}$	79
5.5	Magnitude of E-field distribution in the ellipsoid DMDR for (a) the odd mode and (b) the even mode. Shown here are the top views of the ellipsoid DMDR placed in EMOEW.	80
5.6	Setup for extraction of f_{so} and f_{se} of ellipsoid DMDR in HFSS.	80

5.7	Simulated S_{11} responses with frequency for odd-mode setup, even-mode setup and the setup for extraction of f_{so} and f_{se} of ellipsoid DMDR.	81
5.8	Coupling scheme model of the proposed two pole dual-mode filtering antenna.	81
5.9	Variations of Q_{So} and Q_{Se} with L_S	82
5.10	(a) Circuit representation of DR_o and radiating aperture. (b) Equivalent resonator representation of DR_o with radiating aperture.	83
5.11	(a) Circuit representation of DR_e and radiating aperture. (b) Equivalent resonator representation of DR_e with radiating aperture.	83
5.12	Setup for eigenmode solution in HFSS.	83
5.13	Variations of Q_{oA} and Q_{eA} with L_L	84
5.14	Comparison of the simulated response of filtering antenna to the responses obtained from the coupling parameters for different values of K_{SA}	84
5.15	Photographs of the fabricated L-shaped dual-mode filtering antenna: (a) Cross-sectional view with top-cover removed. (b) Composite view of the filtering antenna with WR-112 coax-to-waveguide adapter.	85
5.16	(a) Frequency response of the proposed filtering antenna. (b) S_{11} response of the filtering antenna showing two poles.	85
5.17	Shown here are the simulated variations of realized gain response for controlling f_{TZ1} and f_{TZ2} with D_2 and D_1 , respectively.	86
5.18	Variations of radiation efficiency with frequency.	87
5.19	(a) Schematic of an EMOEW fed by a propagating-mode WR-112 waveguide and (b) its simulated S_{11} response.	88
5.20	Radiation patterns of filtering antenna at f_0 in (a) E-plane and (b) H-plane.	89
5.21	Simulated variations of f_0 and realized gain with temperature.	90

A.1	Comparison of the simulated response of filtering antenna to the responses obtained from the coupling parameters for different values of K_{SA}	103
A.2	$ S_{21} $ response obtained using the coupling parameters ((A.9a) - (A.9f)) extracted from the simulated model of the filtering antenna, with $K_{SA} = 0$	104
A.3	Shown here are the constant $ S_{21} $ responses obtained from different values of K_{SA} , when all the other parameters ((A.9a) - (A.9f)) in the coupling scheme model are set to zero. Also shown is the $ S_{21} $ response obtained using the coupling parameters (A.9a) extracted from the simulated model of the filtering antenna, with $K_{SA} = 0$	104
A.4	$ S_{21} $ responses obtained from the coupling scheme model for different values of K_{SA} . The values of other parameters in the coupling scheme model are given in (A.9a) - (A.9f).	105

List of Tables

2.1	Comparison of Waveguide Filtering Antennas	32
3.1	Lengths of screws for all three states	45
3.2	Parameters of RFA for all three states	47
3.3	Comparison of Reconfigurable Filtering Antennas	51
4.1	Stopband Bandwidths of Filtering Antenna	70
4.2	Filtering Antenna Parameters at Different Temperatures	72
4.3	Comparison of Filtering Antennas based on Waveguides	73
5.1	Comparison of Waveguide Filtering Antennas	90